Chinese Chemical Letters 33 (2022) 912–915

Contents lists available at ScienceDirect

Chinese Chemical Letters

journal homepage: www.elsevier.com/locate/cclet

Boosted activity of Cu/SiO_2 catalyst for furfural hydrogenation by freeze drying

Hong Du[a], Xiuyun Ma[a], Miao Jiang[a], Z. Conrad Zhang[a,b,*]

[a] Dalian National Laboratory for Clean Energy, Dalian Institute of Chemical Physics, Chinese Academy of Sciences, Dalian 116023, China
[b] State Key Laboratory of Catalysis, Dalian Institute of Chemical Physics, Chinese Academy of Sciences, Dalian 116023, China

ARTICLE INFO

Article history:
Received 9 April 2021
Revised 25 May 2021
Accepted 28 June 2021
Available online 7 July 2021

Keywords:
Freeze drying
Cu/SiO_2
Furfural
Furfuryl alcohol
Hydrogenation

ABSTRACT

The biomass valorization is of great importance as an alternative for the production of transport fuels and fine chemicals. Furfural hydrogenation to furfuryl alcohol is a prevailing industrial route for the utilization of hemicellulose component of biomass. The toxicity of the chromium species in commercial copper chromite catalyst for furfuryl alcohol production motivates the development of efficient chromium-free catalyst. Thus, a highly efficient silica supported copper catalyst is developed in this study. The catalyst is prepared by freeze drying of a gel precursor that is synthesized by ammonia evaporation, followed by calcination and H_2 reduction. The catalyst exhibits higher furfural hydrogenation activity than oven dried catalyst, commercial copper chromite catalyst and a plant supplied commercial silica supported copper catalyst. The catalyst also shows good stability. The superior performance of the freeze dried catalyst has resulted from its developed pore structure and higher amount of Cu^0 as well as Cu^+ active sites.

The rapid consumption of fossil resources and carbon emission derived environmental issues motivate the application of renewable resources. Biomass is a kind of abundant and renewable carbon containing material. The utilization of biomass is an alternative for the production of transport fuels and fine chemicals [1,2]. Furfural (FF) production from biomass by acid-catalyzed dehydration of xylose is a major commercial process for the biomass valorization. As summarized in Fig. 1a, FF is used for the manufacture of furfuryl alcohol (FA), 2-methylfuran (MF), tetrahydrofurfuryl alcohol (THFA), 2-methyltetrahydrofuran (MTHF) and so on [3,4]. FA is widely used as a raw material for the production of foundry resins, plastics, synthetic fibers and other fine chemicals [5]. Due to the extensive applications, FA production accounts for more than 65% of FF produced [6]. Thus, hydrogenation of FF to FA is one of the most valuable and practical routes.

Copper chromite is a commonly used commercial catalyst for the catalytic conversion of FF to FA [7]. The toxic chromium species is harmful to humans and the environment. Thus, the development of chromium-free catalyst attracts vast attention both from academia and industry. Several non-chromium catalysts have been developed for both gas phase and liquid phase hydrogenation processes, such as Ru, Pd, Pt, Cu, Ni [8,9]. The copper based catalyst has been considered as the most promising for industrial application [10]. Recently, we reported that FF was hydrogenated to FA in the gas phase with higher stability by using ammonia evaporation derived silica supported copper catalyst and impregnation derived ethanolamine modified silica supported copper catalyst [10,11]. Besides, ammonia evaporation derived silica supported copper catalysts have been reported to have good performances for ester hydrogenation, CO_2 hydrogenation and FF hydrogenolysis to MF [12-14]. However, the gas phase hydrogenation technology for FF conversion needs more fixed investment in industrial scale production, which limits its application at present. In contrast, the liquid phase hydrogenation is extensively used in plants thanks to its simple process and low fixed input for same scale of capacity.

Thus, an efficient silica supported copper catalyst for FF hydrogenation in liquid phase is developed in the present study. The catalyst (Cu/SiO_2-FD) is synthesized by ammonia evaporation using freeze drying (FD) technology during the preparation process. The performance of Cu/SiO_2-FD is superior to that of conventional ammonia evaporation using oven drying derived catalyst (Cu/SiO_2), commercial copper chromite catalyst purchased from Strem Chemicals (CuCr-S) and a commercial copper catalyst supplied by FA production plant (CuSi-C). The promotion effect of freeze drying on the catalytic performance is also explained by various characterization results.

The detailed information of materials, catalyst preparation, catalyst characterization, catalyst evaluation, product analyses and

* Corresponding author.
E-mail address: zczhang@yahoo.com (Z.C. Zhang).

https://doi.org/10.1016/j.cclet.2021.06.082
1001-8417/

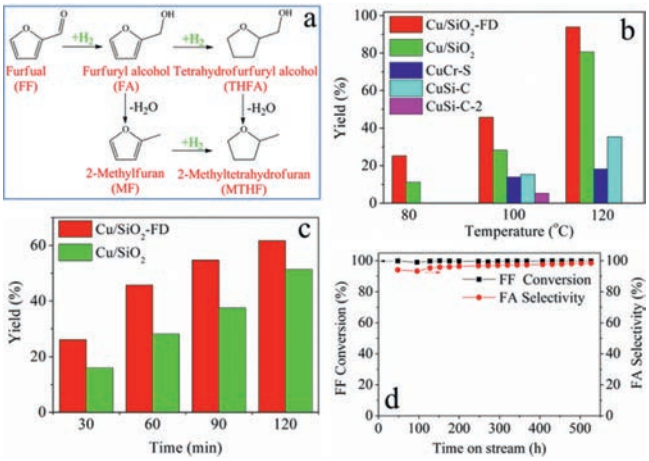

Fig. 1. (a) FF hydrogenation chart. (b) Catalytic performance of Cu/SiO_2-FD catalyst and reference catalysts at different reaction temperature (0.05 g catalyst, 2 g FF and 30 mL 1,4-dioxane, 4 MPa H_2, 600 rpm, 1 h). (c) Catalytic performance of Cu/SiO_2-FD and Cu/SiO_2 at different reaction time (0.05 g catalyst, 2 g FF and 30 mL 1,4 dioxane, 100 °C, 4 MPa H_2, 600 rpm). (d) Stability test of Cu/SiO_2-FD using trickle bed reactor (120 °C, 4 MPa H_2, 2 g FF-1,4-dioxane/g-catalyst/h, H_2/FF = 40).

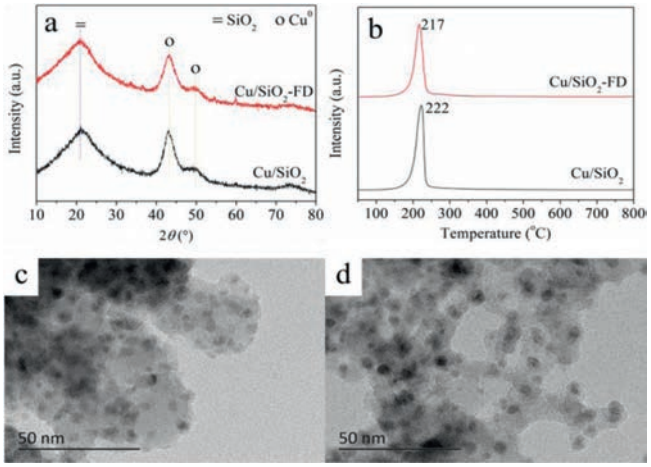

Fig. 2. (a) XRD patterns of freshly reduced samples. (b) H_2-TPR profiles of calcined samples. TEM images of fresh samples for Cu/SiO_2 (c) and Cu/SiO_2-FD (d).

some characterization results are described in Supporting information.

Fig. 1b shows the FF hydrogenation performances over the Cu/SiO_2, Cu/SiO_2-FD and reference commercial catalysts. The selectivity to FA is nearly 100% in all cases. The Cu/SiO_2-FD exhibits higher FA yield at 80 °C, 100 °C and 120 °C compared to Cu/SiO_2. And the activity of Cu/SiO_2-FD is much higher than that of commercial CuCr-S catalyst and CuSi-C catalyst. For the commercial CuSi-C catalyst on the equal copper amount of Cu/SiO_2-FD, its performance as that marked as CuSi-C-2 is considerably far inferior to that of the Cu/SiO_2-FD. Take the Cu/SiO_2 and Cu/SiO_2-FD for comparison (Fig. 1c), FA yield increases with the increasing of reaction time, the Cu/SiO_2-FD performs better than Cu/SiO_2 in all cases. The performance of Cu/SiO_2-FD catalyst is also superior to majority of the copper based catalysts that were reported previously (Table S1 in Supporting information). And the composition of the Cu/SiO_2-FD is much simpler compared to the reference catalysts summarized in Table S1. The stability of the Cu/SiO_2-FD was further assessed using a trickle bed reactor in continuous mode, and the result is depicted in Fig. 1d. There is no obvious decrease of FF conversion and FA selectivity during the whole reaction (~550 h). The above results demonstrate that the silica supported copper catalyst prepared by ammonia evaporation using freeze drying as drying technology (Cu/SiO_2-FD) is more active than that of the silica supported copper catalyst synthesized by ammonia evaporation using conventional oven drying (Cu/SiO_2), commercial CuCr-S catalyst and commercial CuSi-C catalyst supplied by a FA plant. And the Cu/SiO_2-FD catalyst shows excellent stability. Therefore, the freeze drying promotes the performance of silica supported copper catalyst for FF hydrogenation in liquid phase.

To better explain the remarkable effect of freezing drying on the performance, detailed physicochemical characterizations were conducted. As shown in Fig. S1a (Supporting information), the diffraction peaks at 31.0°, 35.6°, 57.1°, 63.3° and 72.0° are observed for both of the calcined Cu/SiO_2-FD and Cu/SiO_2 samples. These characteristic diffraction peaks correspond to the formation of copper phyllosilicate [11,15]. The vibrations of 673 cm^{-1} and 1033 cm^{-1} in fourier transform infrared spectroscopy (FT-IR) spectra (Fig. S1b in Supporting information) of calcined sample verify the existence of copper phyllosilicate [15,16]. The existence of copper phyllosilicate is also verified by the transmission electron microscope (TEM) images (Figs. S1c and d in Supporting information), in which the lamellar structure is observed. Based on the results of XRD, FT-IR and TEM, the copper phyllosilicate exists in both of the calcined Cu/SiO_2 and Cu/SiO_2-FD catalysts.

As listed in Table 1, the copper loading determined by ICP is 17.4 wt% and 17.3 wt% for Cu/SiO_2 and Cu/SiO_2-FD, respectively. The S_{BET}, V_P and D_P of SiO_2 support are 190 m^2/g, 0.46 cm^3/g and 9.4 nm. The S_{BET} and V_P of Cu/SiO_2 increase to 416 m^2/g and 0.82 cm^3/g. A similar increase was reported for ammonia evaporation derived silica supported copper catalyst that contained copper phyllosilicate [17,18]. Surprisingly, the V_P and D_P of calcined Cu/SiO_2-FD are 1.87 cm^3 and 14.3 nm, which are much higher than that of calcined Cu/SiO_2. The S_{BET} (449 m^2/g) of Cu/SiO_2-FD is a little higher than that of Cu/SiO_2 as well. The observation means that freeze drying promotes the pore expansion during the preparation. The S_{BET} and V_P of fresh Cu/SiO_2 and Cu/SiO_2-FD samples decrease due to the decomposition of phyllosilicate during the reduction [19]. However, the V_P and D_P of fresh Cu/SiO_2-FD are also higher than that of fresh Cu/SiO_2. The higher V_P and D_P might be beneficial to the mass transfer, which leads to the higher activity. The similar loosely packed platelet structure and higher methane dry reforming performance of freeze dried $Ni/MgAlO_X$ catalyst compared to oven dried sample was reported previously [20].

As shown in Fig. 2a, the diffraction peaks (2θ = 43.2° and 50.2°) ascribing to Cu^0 are observed in the XRD patterns of freshly reduced catalysts [21]. The average particle size of Cu^0 determined by Scherrer equation is 4.2 nm and 3.5 nm for Cu/SiO_2 and Cu/SiO_2-FD, respectively. The small average particle size of the copper in Cu/SiO_2-FD compared to Cu/SiO_2 is also verified by particle size distribution histograms (Fig. S2 in Supporting information). Moreover, the copper particles are distributed uniformly on the silica support after reduction (Figs. 2c and d). From the H_2-temperature programmed reduction (H_2-TPR) profile (Fig. 2b), it can be seen that the H_2 consumption peak of Cu/SiO_2-FD is slightly lower than that of Cu/SiO_2. This reveals that the calcined Cu/SiO_2-FD is easier to reduce than Cu/SiO_2, which indicates that freeze drying decreased the size of copper particles [22]. Accordingly, copper particles with relatively small size were formed in the fresh Cu/SiO_2-FD.

The Cu 2p and Cu LMM X-ray auger electron spectroscopy (XAES) spectra (Figs. S3A and B in Supporting information) of freshly reduced samples were collected *in-situ* by near ambient pressure X-ray photoelectron spectroscopy (XPS) instrument to analyze the copper state. As listed in Fig. S3A, the peak of Cu $2p_{3/2}$ at about 932.3 eV and a peak of Cu $2p_{1/2}$ at around 952.1 eV are observed. These peaks are assigned to Cu^0 or Cu^+

Table 1
Textural properties of the copper catalysts.

Sample	Cu loading[a] (wt%)	Calcined sample[b]			Fresh sample[c]		
		S_{BET} (m^2/g)	V_p (cm^3/g)	D_p (nm)	S_{BET} (m^2/g)	V_p (cm^3/g)	D_p (nm)
SiO_2	-	190	0.46	9.4	190	0.46	9.4
Cu/SiO_2	17.4	416	0.82	6.6	361	0.73	7.6
Cu/SiO_2-FD	17.3	449	1.87	14.3	362	1.48	16.0

[a] Determined by ICP-OES.
[b] Textural parameters of calcined samples determined using the N_2-physisorption.
[c] Textural parameters of fresh samples determined using the N_2-physisorption. The fresh sample was derived from the reduction of calcined sample. The detailed information is described in Supporting information.

Table 2
Physicochemical properties of the copper catalysts.

Catalyst	D_{Cu}[a](%)	S_{Cu}[a](m^2/g)	d_{Cu}[a](nm)	d_{Cu}[b](nm)	S_{Cu^+}[c](m_2/g)
Cu/SiO_2	28.4	31.9	3.5	4.2	63.6
Cu/SiO_2-FD	43.6	48.8	2.3	3.5	78.6

[a] Copper dispersion, exposed metallic copper surface area and copper particle size were determined using N_2O-titration.
[b] Average Cu particle size was calculated using the Scherrer equation.
[c] Exposed Cu^+ surface area was determined by N_2O titration and *in-situ* XPS.

species [23]. The existence of these peaks suggests that the Cu^+ or Cu^0 formed during the reduction of calcined samples. Since the Cu 2p binding energy (BE) of Cu^+ and Cu^0 are almost identical from XPS spectra, the modified Auger parameter (Table S2 in Supporting information) is used to distinguish the Cu^+ and Cu^0 [24]. The modified Auger parameter equal to the sum of the Cu $2p_{3/2}$ BE and the kinetic energy (KE) of Cu LMM Auger electron. As seen from Table S2, the Cu^+ content in Cu/SiO_2-FD is lower than Cu/SiO_2.

N_2O titration was applied for the measurement of the exposed Cu^0 sites, the results are listed in Table 2. The surface area of metallic copper (S_{Cu}) is 31.9 m^2/g and 48.8 m^2/g for Cu/SiO_2 and Cu/SiO_2-FD, respectively. The Cu^0 dispersion (D_{Cu}) of Cu/SiO_2-FD is higher than Cu/SiO_2. The result reveals that the freeze drying promoted the dispersing of metallic copper. The particle size of metallic copper was calculated based on the N_2O titration and XRD patterns. Relative small metallic copper particles were obtained when the freeze drying was used. Besides, the exposed Cu^+ surface area (S_{Cu^+}) is also calculated based on the Cu^+ content and S_{Cu}. Higher amount of exposed Cu^+ sites are also obtained in the Cu/SiO_2-FD sample. Then, the higher amount of Cu^0 sites and higher amount of Cu^+ sites gave rise to the higher activity of Cu/SiO_2-FD.

The characterization results of calcined samples (Fig. S1 in Supporting information and Table 1) illustrate that the copper phyllosilicate existed in both of Cu/SiO_2 and Cu/SiO_2-FD samples, and the freeze drying promotes the pore expansion. The particles are uniformly distributed in the reduced samples (Fig. 2). The XRD, TEM, H_2-TPR, *in-situ* XPS and N_2O titration results (Fig. 2, Fig. S2, Table 2 and Table S2) suggest that the application of freeze drying during the preparation process promoted the dispersion of copper. Consequently, a relatively higher metallic copper surface area and Cu^+ surface area were obtained. The Cu^0 and Cu^+ species were resulted from the reduction of highly dispersed CuO and copper phyllosilicate under the moderate conditions, respectively. As stated by the previous studies, the synergistic effect of Cu^0 and Cu^+ leads to the conversion of FF to FA [25-27]. In detail, H_2 is adsorbed and activated at the Cu^0 sites to form active H, the C=O bond in FF molecule is adsorbed at the Cu^+ site and polarized through the oxygen electron lone pair. The active H attack the adjacent polarized C=O species. Then, the FF is hydrogenated to FA. Thus, the Cu/SiO_2-FD exhibits the better performance due to its higher amount of Cu^0 and Cu^+ active sites. And the large V_P and D_P also facilitate the reaction by promoting the mass transfer.

In summary, the silica supported copper catalyst prepared by ammonia evaporation using freeze drying technology exhibits the better performance for FF hydrogenation in liquid phase than that of conventional ammonia evaporation using oven drying derived catalyst and representative commercial catalysts. The freeze drying promotes the copper dispersion, which leads to a higher amount of Cu^0 and Cu^+ active sites. In addition, the freeze drying also promotes the pore expansion, which boosts the mass transfer. Thus, the Cu/SiO_2-FD exhibits the superior performance thanks to its higher number of active sites and developed pore structure.

Declaration of competing interest

There are no conflicts of interest to declare.

Acknowledgments

This work was supported by the National Natural Science Foundation of China (Nos. 21721004, 21808217, 21932005), Natural Science Foundation of Liaoning Province (No. 2020-MS-018), Dalian Young Star of Science and Technology Project (No. 2020RQ023) and Dalian Institute of Chemical Physics (Nos. DICP ZZBS201812, DICPI201936).

Supplementary materials

Supplementary material associated with this article can be found, in the online version, at doi:10.1016/j.cclet.2021.06.082.

References

[1] H. Du, X. Ma, M. Jiang, P. Yan, Z.C. Zhang, Energy 221 (2021) 119837.
[2] Z. Zhang, X. Tong, H. Zhang, Y. Li, Green Chem. 20 (2018) 3092–3100.
[3] K. Yan, G. Wu, T. Lafleur, C. Jarvis, Renew. Sust. Energ. Rev. 38 (2014) 663–676.
[4] W. Gong, C. Chen, H. Wang, et al., Chin. Chem. Lett. 29 (2018) 1617–1620.
[5] Y. Wang, D. Zhao, D. Rodríguez-Padrón, C. Len, Catalysts 9 (2019) 796.
[6] R. Mariscal, P. Maireles-Torres, M. Ojeda, I. Sádaba, M.López Granados, Energ. Environ. Sci. 9 (2016) 1144–1189.
[7] G. Singh, L. Singh, J. Gahtori, et al., Mol. Catal. 500 (2021) 111339.
[8] Y. Nakagawa, M. Tamura, K. Tomishige, ACS Catal. 3 (2013) 2655–2668.
[9] S. Thongratkaew, C. Luadthong, S. Kiatphuengporn, et al., Catal. Today 367 (2021) 177–188.
[10] H. Du, X. Ma, M. Jiang, P. Yan, Z.C. Zhang, Appl. Catal. A: Gen. 598 (2020) 117598.
[11] H. Du, X. Ma, P. Yan, et al., Fuel Process. Technol. 193 (2019) 221–231.
[12] Y. Zhao, Y. Zhang, Y. Wang, et al., Appl. Catal. A: Gen. 539 (2017) 59–69.
[13] Z. Wang, Z. Xu, S. Peng, et al., ACS Catal. 5 (2015) 4255–4259.
[14] F. Dong, G. Ding, H. Zheng, et al., Catal. Sci. Technol. 6 (2016) 767–779.
[15] B. Li, L. Li, H. Sun, C. Zhao, ACS Sustain, Chem. Eng. 6 (2018) 12096–12103.
[16] Y. Zhao, S. Li, Y. Wang, et al., Chem. Eng. J. 313 (2017) 759–768.
[17] X. Wang, M. Chen, X. Chen, et al., J. Catal. 383 (2020) 254–263.
[18] X. Zheng, H. Lin, J. Zheng, X. Duan, Y. Yuan, ACS Catal. 3 (2013) 2738–2749.
[19] H. Du, X. Ma, M. Jiang, et al., Catal. Today 365 (2021) 265–273.
[20] J. Huang, Y. Yan, S. Saqline, W. Liu, B. Liu, Appl. Catal. B: Environ. 275 (2020) 119109.

[21] Z. Wang, Z. Xu, M. Zhang, et al., RSC Adv. 6 (2016) 25185–25190.
[22] C. Chen, L. Lin, R. Ye, et al., Fuel 290 (2021) 120083.
[23] J. Zheng, J. Zhou, H. Lin, et al., J. Phys. Chem. C 119 (2015) 13758–13766.
[24] X. Han, Q. Zhang, F. Feng, et al., Chin. Chem. Lett. 26 (2015) 1150–1154.
[25] S. Chen, R. Wojcieszak, F. Dumeignil, E. Marceau, S. Royer, Chem. Rev. 118 (2018) 11023–11117.
[26] R. Ye, L. Lin, Q. Li, et al., Catal. Sci. Technol. 8 (2018) 3428–3449.
[27] F. Hao, J. Zheng, S. He, et al., Catal. Commun. 151 (2021) 106266.